Construction of human single-chain variable fragment antibodies of medullary thyroid carcinoma and single photon emission computed tomography/computed tomography imaging in tumor-bearing nude mice

QIONG LIU[1], HUA PANG[1], XIAOLI HU[2], WENBO LI[1], JIMEI XI[1], LU XU[1] and JING ZHOU[1]

[1]Department of Nuclear Medicine, The First Affiliated Hospital of Chongqing Medical University;
[2]Department of Radiology, The First Affiliated Hospital of Luzhou Medical College, Chongqing, P.R. China

Received July 14, 2015; Accepted September 4, 2015

DOI: 10.3892/or.2015.4345

Abstract. Medullary thyroid carcinoma (MTC) is a rare tumor of the endocrine system with poor prognosis as it exhibits high resistance against conventional therapy. Recent studies have shown that monoclonal antibodies labeled with radionuclide have become important agents for diagnosing tumors. To elucidate whether single-chain fragment of variable (scFv) antibody labeled with ^{131}I isotope is a potential imaging agent for diagnosing MTC. A human scFv antibody library of MTC using phage display technique was constructed with a capacity of $3x10^5$. The library was panned with thyroid epithelial cell lines and MTC cell lines (TT). Western blotting and enzyme-linked immunosorbent assay (ELISA) were used to identify the biological characteristics of the panned scFv. Methyl thiazolyl tetrazolium (MTT) assay was also used to explore the optimal concentration of the TT cell proliferation inhibition rate. They were categorized into TT, SW480 and control groups using phosphate-buffered saline. Western blotting showed that molecular weight of scFv was 28 kDa, cell ELISA showed that the absorbance of TT cell group was significantly increased (P=0.000) vs. the other three groups, and MTT assay showed that the inhibition rate between the two cell lines was statistically significantly different (P<0.05) when the concentration of scFv was 0.1, 1 and 10 μmol/l. The tumor uptake of ^{131}I-scFv was visible at 12 h and clear image was obtained at 48 h using the single photon emission computed tomography. scFv rapidly and specifically target MTC cells, suggesting the potential of this antibody as an imaging agent for diagnosing MTC.

Correspondence to: Dr Hua Pang, Department of Nuclear Medicine, The First Affiliated Hospital of Chongqing Medical University, Chongqing, P.R. China
E-mail: phua1973@163.com

Key words: phage antibody library, human single-chain variable fragment, medullary thyroid carcinoma, screening, SPECT imaging

Introduction

Medullary thyroid carcinoma (MTC) is a rare, but aggressive neuroendocrine tumor that arises from calcitonin (CT)-producing parafollicular cells (C cells) of the thyroid, and accounts for 5-8% of all thyroid cancers (1,2). Based on the germline RET gene mutation status and clinical phenotype, MTC can be classified as 'sporadic' (75%) or 'hereditary' (25%) (3). It has a slow but progressive clinical course with an early involvement of lymph nodes. It is challenging to diagnose MTC in clinical practice. Use of fine-needle aspiration cytology is helpful in diagnosing cancer including MTC, but some results of this technique are indeterminate, benign or have inadequate cytological studies (4-9); a major difficulty is in obtaining sufficient tumor tissue. Also, ultrasonography is frequently 'not suspicious' in diagnosing MTC (10-16). Thyroid C cells produce and secrete CT, which is a more specific circulating marker and is widely used for diagnosis and monitoring. Nevertheless, the issue of screening serum CT in patients with thyroid nodules is partially unsettled due to analytical problems, low prevalence of MTC, increased cost of routine determination and risk of inappropriate surgery after misleading diagnosis (17). MTC cannot be treated using radionuclide therapy as it does not fulfill the necessary conditions. Also, it is not sensitive to radiotherapy. Surgery is the main and only effective treatment, with total thyroidectomy plus cervical lymph node dissection and should be performed before the occurrence of distant metastasis (18). Hence, there is an urgent need to develop accurate and non-invasive methods for early diagnosis of MTC.

Monoclonal antibodies that recognize specific markers expressed on tumor cells have been widely used in the research and diagnosis of cancer. Anti-carcinoembryonic antigen monoclonal antibody was successfully used in tumor imaging in 1978 (19). However, the use of murine antibodies, which are produced using hybridoma technique, in large intact antibodies in solid tumors is limited by the response of human anti-murine antibody (HAMA) (20), thereby weakening the effectiveness of the treatment. In 1988, a single-chain fragment of variable (scFv) antibody was first constructed using genetic fusion of variable regions of the heavy (VH) and light

chains (VL) (21). The following year, surface display phage antibody library was established. The phage antibody not only can identify and bind the corresponding antigen, but also can infect the host bacteria for amplification. Sufficient amounts of heterologous proteins are produced by efficient microbial production systems (22,23). Also, scFv has shown distinct advantages as it can be prepared through chemical synthesis at a relatively low cost, is less responsive to HAMA and has rapid blood clearance. Thus, this technique was used to construct single-chain antibody phage libraries for anti-MTC.

Recently, molecular imaging has been widely used for diagnosing solid tumors using positron emission tomography (PET) and single photon emission computed tomography (SPECT) (24,25). Due to their non-invasive character in patients and high specificity to tumor lesions, antibodies against tumor cell-specific surface markers have become an ideal method for tumor imaging. Hence technetium-99m (^{99m}Tc), with a lower energy (140 keV) and shorter half-life, has been widely used in the departments of nuclear medicine worldwide. However, ^{99m}Tc is not the best choice for SPECT imaging due to its limitation in treatment. In contrast, iodine-131 (^{131}I) is easy to obtain, has higher energy (364 keV) and relatively long half-life (8 days). Moreover, ^{131}I not only can emit γ-ray for imaging but also can emit β-rays for treatment. Pavlinkova *et al* reported the use of ^{131}I-labeled scFv in nude mice bearing colon cancer cells and found that the tumors completely subsided with a probability of 60% in the treatment group (25). This may be a new treatment targeting tumors.

In the present study, the phage display technique was used to construct a human single-chain antibody library of MTC. Later, this library was panned with thyroid epithelial cell lines (TECs) and MTC cell lines (TTs). Panned scFv was identified using western blotting and enzyme-linked immunosorbent assay (ELISA). After purification, the scFv was labeled with ^{131}I and SPECT-CT tomography imaging was performed in nude mice bearing TT cells. These results may provide a basis for the future development of diagnosis and therapeutics of MTC.

Materials and methods

Construction and stitching of gene library. Phagemid vector pCANTAB-5E, helper phage M13K07 and *Escherichia coli* TG1 (*E. coli* TG1) were obtained from New England BioLabs (New England). Based on the literature (26,27), polymerase chain reaction (PCR) primers were designed and commissioned by Chongqing MacKay Ltd. (Chongqing, China). Reverse transcription (RT)-PCR reaction synthesis of first-strand complementary DNA (cDNA) was performed based on the instructions in the kit. Later the heavy chain linker (VH-linker) and the light chain linker (VL-linker) were amplified from the cDNA. A sequence encoding E-tag was included in the forward primer. The PCR protocol was as follows: initial denaturation at 94˚C for 5 min, 35 cycles of melting at 94˚C for 30 sec, annealing at 53˚C for 30 sec and extension at 72˚C for 30 sec, 1 cycle at 72˚C for 10 min. The purified PCR products were digested and inserted into the pCANTAB-5E and then transformed into *E. coli* TG1 cells (*E. coli* TG1 was used as the main host for gene cloning and library screening). Transformed *E. coli* TG1 cells were selected from lysogeny broth medium containing ampicillin. PCR amplification was performed according to the instructions of the plasmid extraction kit (purchased from Beijing Hundred Tektronix Biotechnology Co., Beijing, China). The product was subjected to 1.0% agarose gel electrophoresis to identify the rate of insertion of the antibody gene. Positive clone was identified using *Sfi*I and *Not*I double digestion and analyzed using 1.0% agarose gel electrophoresis to identify whether there was visible release of a fragment. The positive plasmid was sequenced by Shanghai Handsome Positive Biotechnology (Shanghai, China).

Preparation and screening of phage antibody library. The transformed *E. coli* TG1 cells were inoculated into 2X YT medium containing 2% (w/v) glucose at 37˚C for 1 h, then M13K07 helper phages were added and oscillated at 250 rpm for 1 h and then centrifuged, and the cells were transferred to fresh 2X YT-AK medium (2XYT containing ampicillin and kanamycin) and were incubated overnight at 37˚C and 250 rpm. The recombinant phages were recovered from the overnight culture and precipitated using polyethylene glycol-NaCl. The phage antibody was panned with TEC for blocking non-specific binding sites of the antibody, then unbounded phage was added to the immune-coated tube, which has been coated with TT cells, rocked gently in a warm bath for 1.5 h, then allowed to rest for 30 min and the supernatant was removed. Cells were gently washed thrice using phosphate-buffered saline (PBS) with Tween-20 (PBST) and PBS followed by elution using 0.2 M glycine-HCl (pH 2.5) and neutralized using Tris-HCl (pH 7.5). Recombinant phages were transformed into *E. coli* TG1 cells [optical density (OD), 0.6] and plated on 2X YT-A medium at 37˚C for 1 h. The bacteria were next cultured in 2X YT-AK medium supplemented with $4x10^{10}$ pfu/mol M13K07 helper phages at 37˚C overnight. Overnight bacteria solution was centrifuged at 10,000 rpm for 20 min and the supernatant was removed. Thus, the first round of panning was completed. The next four rounds of panning were identical to the first except that washing was more stringent (5X PBST and 5X PBS). A small amount of antibody library before and after the screening was taken to infect *E. coli* TG1 cells in SOBAG agar plates to calculate the titer of antibody library and input-output ratio, as an enriched index of specific phage antibodies.

Phage ELISA and scFv ELISA detect recombinant antibodies. Phage ELISA and scFv ELISA were used to detect the presence of M13K07 helper phages and E-tagged scFv (the transformed *E. coli* TG1 cells injected with M13K07 helper phages and pCANTAB-5E contain a sequence encoding for a peptide E-tag and thus yield E-tagged scFv). In phage ELISA, the supernatant of the fifth screening in the previous step was added to the TT cells in well-packaged microtiter plates as the first antibody. In scFv ELISA, the transformed *E. coli* TG1 cells were induced using 1 mM isopropyl-β-D-thiogalactopyranoside (IPTG). Under these conditions, soluble scFv was released into the growth medium where it can be used for detection. Soluble scFv was added to the TT cells in well-packaged microtiter plates as the first antibody. The control group was established by the addition of PBS. Horseradish peroxidase (HRP)/anti-M13 monoclonal antibody and HRP/anti-E-tag monoclonal antibody (both from Abcam Company, Shanghai, China) were added to each well

for secondary antibody. 3,5,5-Tetramethyl benzidine dihydrochloride (TMB) was added to each well and kept in dark for 45 min. A stop solution was added and the reading was obtained in the ELISA reader at 450 nm.

Expression and purification of scFv. A few phage clones that underwent reaction with the TT cells using ELISA were selected and transferred into *E. coli* HB2151 (New England BioLabs). Transformed cells were inoculated into the SOBAG-N medium containing nalidixic acid at 30˚C overnight. The cells were transferred into a fresh 2X YT-AI medium containing IPTG and collected using centrifugation when the shock time was 4 and 6 h, respectively. The cells were resuspended in PBS, frozen in liquid nitrogen for 30 min and thawed at 37˚C. Ultrasound was used to break down bacteria after freezing and thawing thrice. The resulting supernatant was collected using centrifugation and contained soluble scFv from whole cells. Soluble scFv was purified using HiTrap™ anti-E-tag column. Each tube was monitored at A_{280nm} and a few tubes were collected at the highest OD value of A_{280nm}. This results in the purified production of soluble antibodies. Purified soluble scFv was stored at 4˚C for further use.

Sodium dodecyl sulfate-polyacrylamide gel electrophoresis and western blotting. To examine the expression of scFv, the supernatant from the uninduced and induced culture at 4 and 6 h of the recombinant clone in *E. coli* HB2151 was obtained. Purified soluble scFv was run on sodium dodecyl sulfate-polyacrylamide gel electrophoresis (SDS-PAGE), followed by Coomassie brilliant blue. *E. coli* HB2151 induced at 4 and 6 h was run on SDS-PAGE with uninduced *E. coli* HB2151 as the control group, then transferred onto nitrocellulose membrane followed by blocking with MPBS (2% skim milk in PBS) for 1 h at room temperature with gentle shaking. After washing, the membrane was incubated with the HRP-mouse anti-E-tag monoclonal antibody as the first antibody and HRP-anti-mouse antibody as the secondary antibody. It underwent chemiluminescence, then developed and fixed.

Cell ELISA detection of soluble antibodies immune activity. TT cells, TEC, and SW480 cells were cultured into 96-well plates at 37˚C for 48 h, then cells were washed thrice with PBS, dried by placing the cells in the incubator, and fixed with 0.25% glutaraldehyde for 10 min. After blocking and washing, cells were washed thrice with PBST and PBS, respectively. To each 96-well plate, purified soluble recombinant antibodies were added. HRP/anti-E-tag monoclonal antibody was used as the secondary antibody (1/10,000 dilution, 37˚C, 1 h). PBS was used instead of purified scFv TT cells as the blank control group. TMB was added to each plate and kept in the dark for 45 min. Reading was obtained in the ELISA reader at 450 nm, and photographed using light microscopy.

Methyl thiazolyl tetrazolium assay exploring the inhibition of the proliferation rate. TT and SW480 cells were grown in 96-well plates. Serial dilutions of scFv solution at concentrations of 10^{-4}, 10^{-3}, 10^{-2}, 10^{-1}, 1 and 10 μmol/l (50 μl/well) were added to each 96-well plate the next day, PBS was added to the control group and five replicate wells were set in each group. After these cells were incubated in a cell incubator for 48 h, MTT solution was added (20 μl/well) for 4 h, then the reaction was terminated and later dimethyl sulfoxide (150 μl/well) was added to each well. After low temperature shock for 10 min, reading was obtained in the absorbance microplate reader at A_{490nm} and then the inhibition rate was calculated. Inhibition rate (%) = (control group A - experimental group A)/(control group A) x %.

Radiolabeling, purification and radiochemical purity test. ^{131}I was labeled using a modification of the chloramine-T method. Briefly, soluble scFv was added to freshly prepared ^{131}I, chloramine-T solution was added 3 min later and 200 μl potassium iodide was then added 1 min later to stop the reaction. This solution was purified using Sephadex G-200 and filter sterilized. Labeling efficiency was measured using trichloroacetic acid precipitation. Paper chromatography was used to determine the radiochemical purity of ^{131}I-scFv and to calculate the specific activity of radioactivity. Purified ^{131}I-scFv was added to the fresh human serum (obtained from the blood bank of the First Affiliated Hospital of Chongqing Medical University, Chongqing, China) at 37˚C for 24 h to test the stability of the serum. Later these were analyzed at 1, 6, 12 and 24 h, using paper chromatography.

Animal models and biodistribution studies. Animal biodistribution experiments and SPECT-CT imaging were performed in 4- to 6-week-old male nude mice (Department of Laboratory Animal Center at Chongqing Medical University), which were xenografted with TT cells. Cells were injected subcutaneously into the right forelimb of the nude mice. After 6 weeks, the diameter of tumors was ~1.0 cm. Twelve tumor-burdened nude mice were divided into four groups, with three in each group. ^{131}I-scFv was injected into the tail veins of nude mice. The animals were sacrificed and dissected at 12 h, 1, 2 and 3 days after the injection of ^{131}I-scFv. Tumor tissues, heart, liver, spleen, lung, kidney, stomach, intestines, brain and muscle were removed and weighed. The radioactivity of the tissues was measured using a γ-counter. Results were expressed as the percentage injected dose/gram of tissue (% ID/g). Ethics approval for the animal studies was given by the First Affiliated Hospital of Chongqing Medical University Biomedical Ethics Committee.

SPECT-CT imaging. Thyroid of nude mice bearing TT cells was sealed using potassium iodide and injected with ^{131}I-scFv. SPECT-CT was used for anteroposterior static imaging (SPECT-CT Symbia T2; Siemens, Germany), using a single head rotating scintillation camera at 12 h, 1, 2 and 3 days after the injection of ^{131}I-scFv to observe the radioactivity in tumor (high-energy collimator, matrix 256x256, peak energy of 364 keV, acquisition time for each frame 15 min). Image fusion was performed using the SPECT-CT when the tumor tissues were clearly visible.

Results

Construction of gene library. The VH and VL genes were amplified from the cDNA derived from the mRNA, which was extracted from the lymph nodes near the MTC tumor tissue, and were visualized on 1% agarose gel as 370- and 350-bp bands, respectively. A 750-bp scFv DNA was produced by assembling VH and VL DNA fragments and was subsequently cloned to

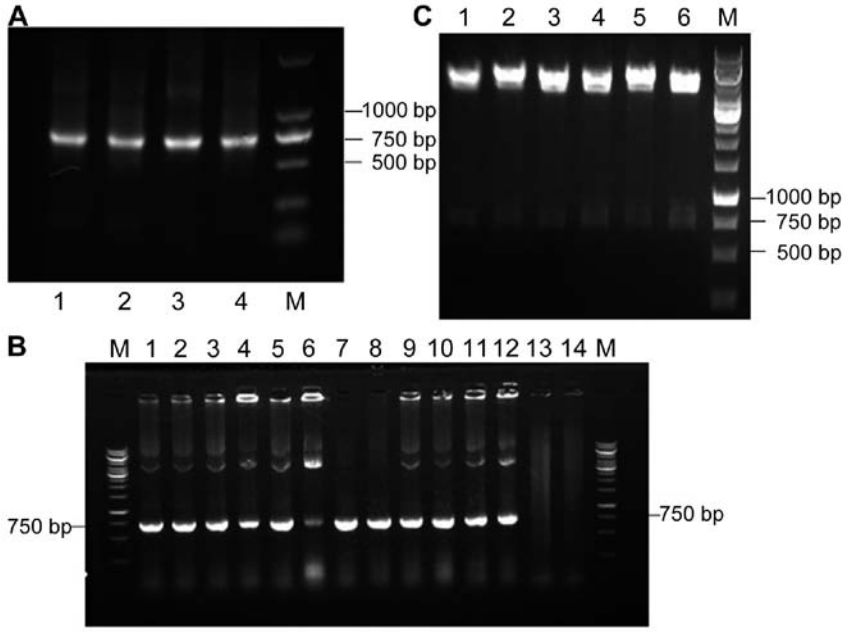

Figure 1. (A) Identification of single antibody gene after link using agarose gel electrophoresis (M, DL2000; lanes 1-4, scFv gene). (B) PCR identification of randomly chosen clone plasmid (M, 1 kb DNA ladder; lanes 1-12, PCR-positive; lanes 13-14, PCR-negative). (C) Double enzyme results of positive clone *Sfi*I and *Not*I [M, 1 kb DNA ladder, lanes 1-6, scFv gene fragment (down) and carrier (up)]. PCR, polymerase chain reaction.

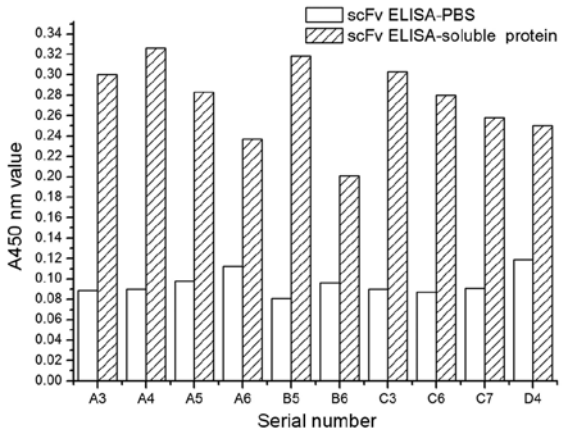

Figure 2. Analysis of the binding activities of the selected soluble scFv against TT cells. ELISA, enzyme-linked immunosorbent assay; PBS, phosphate-buffered saline; scFv, single-chain fragment of variable.

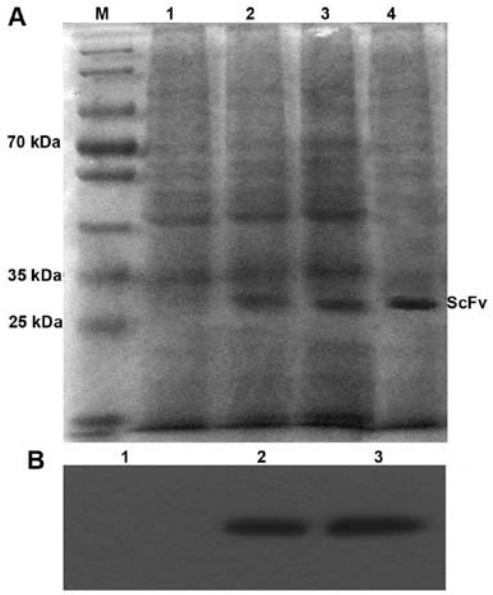

Figure 3. SDS-PAGE and western blot analysis of the scFv expressed in *E. coli* HB2151. (A) M, protein molecular weight marker; lane 1, uninduced *E. coli* HB2151; lane 2, expression of scFv supernatants induced for 4 h; lane 3, expression of scFv supernatants induced for 6 h; lane 4, purified scFv. (B) Detection of purified scFv using western blotting. Lane 1, uninduced *E. coli* HB2151 with a negative result; lane 2, purified scFv induced for 4 h; lane 3, purified scFv induced for 6 h. scFv, single-chain fragment of variable; SDS-PAGE, sodium dodecylsulfate-polyacrylamide gel electrophoresis.

express recombinant E-tag scFv (Fig. 1A). As shown in Fig. 1B, the gene encoding the Dmab (scFv)-Fc antibody was amplified from 12 of the 16 colonies. Six monoclonal plasmids were randomly chosen and double digested using *Sfi*I and *Not*I. The release of the fragment can be observed (Fig. 1C). These results showed that MTC-specific scFv was successfully obtained.

Detection of soluble antigen-positive recombinant antibodies using phage ELISA and scFv ELISA. After five rounds of 'adsorption-elution-amplification', the rates of harvest of the first and the fifth rounds were 1.96×10^{-6} and was 2.84×10^{-4} %, respectively, showing an increase of 145-fold. Anti-MTC antibodies have been significantly enriched. The enriched scFv library was first detected using phage ELISA and then using scFv ELISA; 13 and 10 bacterial clones in 20 showed a positive reaction to TT cells, which were detected using phage ELISA and scFv ELISA with a positive rate of 65 and 50%, respectively. The data also indicated that positive wells corresponding to coding have a high consistency of detection between the two methods, which suggests that phage-infected *E. coli* TG1-induced protein initially showed soluble expression (Fig. 2).

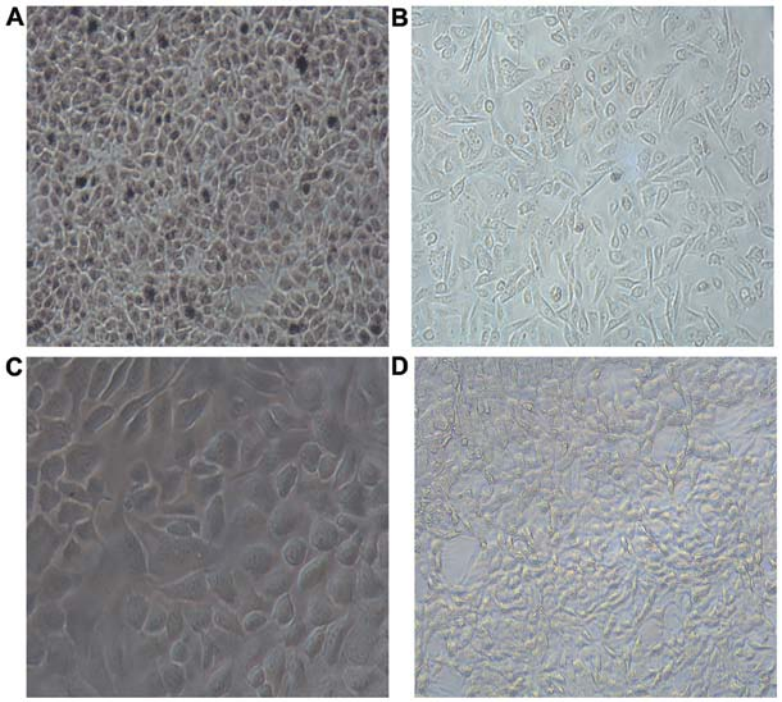

Figure 4. Specific test of purified antibody under microscope (TMB magnification, x200). The binding properties of the purified antibody were tested using cell ELISA assays, where it manifested a very strong binding to TT cells (A). In contrast, no binding to TT cells was observed when the purified antibody was replaced with PBS (D). No binding was detected when the plates were coated with TEC and SW480 cells (B and C). ELISA, enzyme-linked immunosorbent assay; PBS, phosphate-buffered saline; TMB, 3,5,5-tetramethyl benzidine dihydrochloride.

SDS-PAGE and western blotting. HiTrap™ anti-E-tag was used to purify soluble proteins. Five tubes have higher readings at A_{280nm}, and their readings were as follows: (no. 12) 0.1; (no. 13) 0.15; (no. 14) 0.1; (no. 15) 0.09; and (no. 16) 0.05, merging the five tubes that have highest A_{280nm} reading as purified expression of soluble scFv. Fig. 3A and B shows the results of SDS-PAGE followed by Coomassie brilliant blue staining and western blot analyses for the purified scFv proteins. Supernatant of the uninduced *E. coli* HB2151, the induced supernatant 4 and 6 h of the recombinant clone in *E. coli* HB2151, and purified soluble scFv were obtained using SDS-PAGE. Data showed the soluble expression of antibody molecules after the induction of IPTG (Fig. 3A, lanes 2, 3 and 4); soluble proteins were not expressed in lane 1. Western blot analysis showed that for developing clear bands, the relative molecular weight of soluble proteins should be ~28 kDa, indicating the soluble expression of the antibody. The expression levels of the soluble scFv were not significantly increased after being induced for 4 and 6 h.

Detection of soluble scFv immune activity through cell ELISA. Absorbance at A_{450nm} was detected using ELISA. Results of variance analysis showed that the TT cell group (0.41±0.12), TEC group (0.13±0.01), SW480 cell group (0.20±0.03) and PBS group (0.07±0.01) have statistically significant differences (F=103.626, P=0.000). Multiple comparisons showed that the difference between the TT cell and the other three groups were statistically significant (P=0.000). The results showed that the binding ability of scFv to TT cells was significantly higher than that of the other groups, which means scFv has higher specificity in TT cells. Light microscope images showed that scFv has high immune activity (Fig. 4).

Table I. Difference in concentrations of scFv on the inhibition rate of TT and SW480 cells (mean ± standard deviation, %, n=5).

Concentration (μmol/l)	TT cells	SW480 cells	t	P-value
0.0001	0.03±0.32[a]	-0.06±0.17	0.562	0.589
0.001	0.11±0.20[a]	0.02±0.07	0.964	0.362
0.01	0.28±0.23[a]	0.06±0.13	1.992	0.08
0.1	0.31±0.16[ab]	0.10±0.06[b]	2.881	0.02
1	0.43±0.17[ab]	0.04±0.03[b]	5.073	0.006
10	0.59±0.15[ab]	0.08±0.05[b]	7.324	0.000

[a]Statistically significant inhibition rate (P=0.004) in the group at different concentrations of scFv; [b]between the same two cell lines, inhibition rate of concentration of scFv was statistically significant (P<0.05). scFv, single-chain fragment of variable.

Inhibition of cell proliferation test. Difference in concentrations of scFv on the inhibition rate of TT and SW480 cells is shown in Table I. It indicated that inhibition rates tend to increase with the increase in the concentration of drug in the TT cell group. When the concentration of scFv was 0.1, 1 and 10 μmol/l, inhibition rate between the TT and SW480 cell groups at the same concentration was statistically significant, and were t=2.881, P=0.02; t=5.073, P=0.006; and t=7.324, P=0.000. These data indicated that inhibition rate between two groups was different when the concentration was 0.1, 1 and 10 μmol/l, while the inhibition rate was not significantly

Table II. Biodistribution of scFv in the nude mice bearing medullary thyroid carcinoma cells (% ID/g, mean ± standard deviation, n=3).

	12 h	1 day	2 days	3 days
Tumor	4.32±0.12	4.05±1.25	3.58±0.65	2.33±0.11
Blood	5.35±1.21	4.11±1.19	0.83±0.12	0.58±0.07
Liver	10.22±0.57	7.02±1.33	2.41±0.33	1.08±0.11
Kidney	9.01±0.66	7.01±1.52	6.59±0.29	4.00±0.06
Spleen	5.32±0.86	2.33±0.81	1.66±0.72	0.51±0.23
Heart	4.21±1.12	1.65±0.38	0.60±0.72	0.43±0.11
Lung	2.52±1.04	1.32±0.52	0.52±0.66	0.32±0.20
Stomach	3.42±1.25	1.63±1.21	1.18±0.58	0.64±0.02
Intestines	6.66±1.05	4.08±0.87	3.26±0.53	0.94±0.32
Brain	1.22±0.11	0.85±0.12	0.66±0.26	0.32±0.08
Muscle	2.98±0.28	1.45±0.39	0.69±0.32	0.52±0.65

scFv, single-chain fragment of variable.

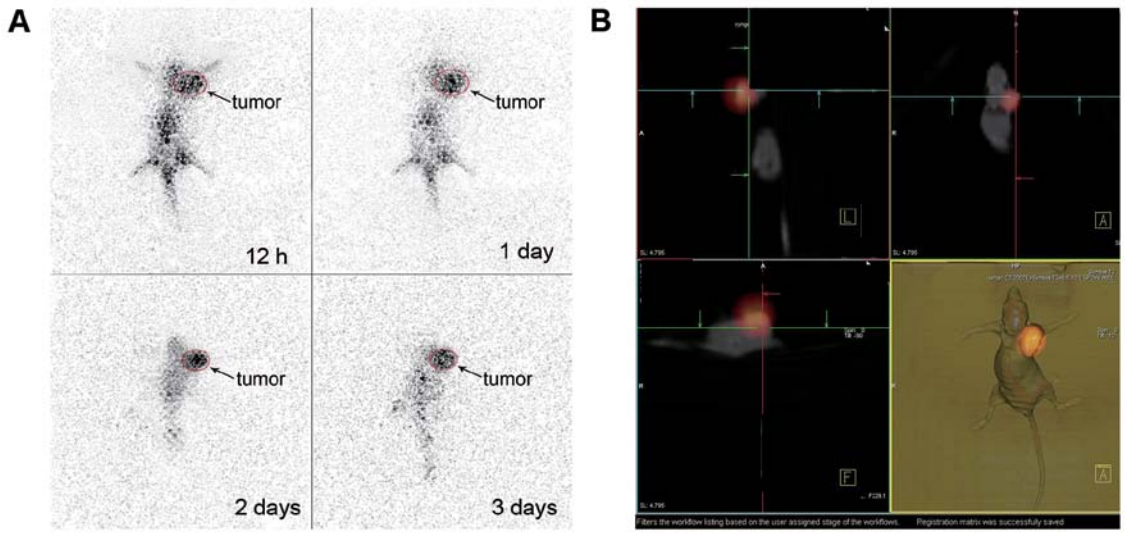

Figure 5. Static SPECT imaging and SPECT-CT fusion imaging. (A) SPECT imaging of nude mouse bearing a tumor after the caudal vein injection of ^{131}I-scFv. (B) SPECT-CT fusion imaging and simulated imaging of nude mouse bearing a tumor at 2 days after the injection of ^{131}I-scFv into the tail veins. CT, computed tomography; scFv, single-chain fragment of variable; SPECT, single photon emission computed tomography.

different in other concentrations. The inhibition rate of TT cells reached the peak with a value of 0.59±0.15% when the concentration of scFv was 10 μmol/l. The comparison between TT cell groups at different concentrations of scFv was statistically significant (F=4.767, P=0.004); pairwise comparison showed no significant differences between 10 and 1 μmol/l groups (P=0.253), but when 10 μmol/l group was compared with other concentrations they were statistically significant (P<0.05). The comparison between SW480 cell groups at different concentrations of scFv did not show statistically significant difference (F=1.666, P=0.181).

Radiolabeling, purification and radiochemical purity test. Results showed that there were two radioactive peaks after chromatography on the Sephadex G-200 column. The first radioactive peak was at fraction 35-45 and the second at fraction 60-68. The first radioactive peak was taken and purified, labeled ^{131}I-scFv. Labeling rate of ^{131}I-scFv was 78.6±0.083%, when measured using trichloroacetic acid. The radiochemical purity of purified ^{131}I-scFv was 87.1±0.78% and specific activity was 2.9±0.32 MBq/μg. After storage at 37˚C in the human blood serum, the radiochemical purities of ^{131}I-scFv at 1, 6, 12 and 24 h were 95.1, 94.2, 93.1 and 92.6%, respectively, showing >90% purity.

Biodistribution studies. Biodistribution data in nude mice with TT cell xenografts are shown in Table II. ^{131}I-scFv was mainly distributed in the blood, liver, kidney and intestines 12 h after the injection. High uptake (% ID/g) was still noted 1 day after the injection. The kidney showed high radioactivity uptake in all the tissues, which indicated that kidney is the primary route of excretion of the label. However, brain tissue showed less distribution, which indicates the difficulty of the drug in crossing the blood-brain barrier. At 12 h after injection,

the tumors accumulated 4.32±0.12% ID/g, which decreased to 2.33±0.11% ID/g at 3 days after the injection, but it still showed a higher uptake (% ID/g) compared with other tissues. ^{131}I-scFv in tumor tissue shows long residence time and slow rate of clearance. The ratio of radioactivity of tumor:blood and tumor:muscle increased with time gradually, reached a peak at 48 h; the tumor:blood ratio was 4.31, whereas, tumor:muscle ratio was 5.19 at the peak of 48 h and, then both decreased.

SPECT imaging. The static SPECT imaging of nude mice bearing human MTC at 12 h, 1, 2 and 3 days after injection of ^{131}I-scFv is shown in Fig. 5A. A high concentration of radioactivity in the tumor tissues is shown, the background at 12 h after the injection of ^{131}I-scFv was relatively high, and radioactivity accumulated mainly in the liver and kidney. At 1 day after administration, a high concentration of radioactivity accumulated in the tumor of the mice, and the background was <12 h. At 2 days, concentration of radioactivity of other body tissues was very low compared with tumor tissues, which showed the outline of tumor tissue very clearly; at this point, rows of SPECT-CT fusion imaging and area of fusion tumor are developing well. Fig. 5B shows the results.

Discussion

Monoclonal antibodies have increasingly become important in the diagnosis and treatment of tumors. Though a variety of anticancer drugs are available, their clinical application is limited due to their failure to distinguish cancer cells from normal cells, which cause toxic adverse effects (28,29). Monoclonal antibodies directly deliver the drug to the tumor, resulting in a high drug concentration in the tumor. Monoclonal antibodies labeled with a radionuclide are ideal vehicles for imaging since they easily reach the tumor due to their small molecular weight and strong penetrating force. In the present study, a human single-chain antibody library of MTC was constructed and special scFv was labeled with ^{131}I. It was hypothesized that ^{131}I-scFv can be a candidate for molecular probes in the non-invasive imaging of tumor angiogenesis. The main finding of the present study was that the new molecular probe preferentially adhered to tumor angiogenesis. The data support the hypothesis that ^{131}I-scFv can selectively accumulate in tumor tissues of nude mice-bearing TT cells, indicating that the ^{131}I-scFv is specific to MTC.

However, the ability to obtain the desired antibody from the antibody library is constrained by many factors including the capacity, diversity amplification, conditions of amplification and screening of antibody library. Among these factors, the most important being the amplification of all the antibody genes, making design and application of a good primer particularly important in increasing the storage capacity and maintaining the diversity of the antibody libraries. Primer design should contain as much of the variable region gene as possible (30). Variable region gene family is mostly common in Vγ3 and Vκ3 types. Linker peptide sequence was also designed in the process assembly of PCR primers, which makes connecting peptide synthesis easier and increases the diversity of the scFv gene. It is important to construct a large antibody library to ensure high-affinity antigen-antibody screening (31,32). Data showed that the capacity of our library is $3x10^5$, which is relatively small compared with the diversity of natural human antibody. Although the size of our library is not large, the quality was enough for use in isolating the anti-MTC antibody. Our libraries were subjected to in-frame selection by fusion with kanamycin and ampicillin resistance selection. The quality was validated using PCR. Gene insertion rate of scFv was 87.5%, which further validates the reliability of the antibody library.

Although classical screening technique could provide successful screening results, it does not mean that the use of screening strategy guarantees successful screening of antibody against any antigens. It can only be used when the nature of the antigen is clear and the antigen can be purified. For antigens such as tissues or cell surface receptors, the cell surface, as well as novel cell surface markers at specific differentiation or disease-induced state. For those screening methods that cannot be purified or are indeterminate, conventional screening method is no longer applicable (33). A number of studies have shown that complex antigen screening can lead to better results in cell, organization and body panning method (34). In the present study, TECs were used as negative selection, thus removing some non-specific phage antibody. Later TT cells acted as complex antigen conditions. After five positive screening, MTC-associated antibody phage was significantly enriched.

Use of ^{131}I-labeled polypeptide is feasible in the present study. Labeling rate of ^{131}I-scFv was 78.6±0.083%, the radiochemical purity of purified ^{131}I-scFv was 87.1±0.78% and the radiochemical purity of ^{131}I-scFv which was stored at 37˚C in human blood serum at 48 h was 92.6%. These results showed that ^{131}I-scFv has good stability *in vitro*, which meets the requirements of *in vivo* experimental studies on peptide. SPECT imaging can directly observe the dynamic changes in the imaging agents in the *in vivo* distribution. Results of ^{131}I-scFv polypeptide imaging showed that in nude mice xenografted with TT cells, dynamic changes in distribution in the imaging agent *in vivo* can be directly observed using the SPECT imaging, which was closer to clinical practice. The selection of radionuclide is a critical factor to consider for ^{131}I-scFv. Results of ^{131}I-scFv *in vivo* imaging of nude mice showed more accumulation of radiotracer in the liver, which was also observed in the biodistribution analysis, the liver fades with time. However, imaging showed a low level of radioactivity in the intestine. Concentrations of radioactivity were not found in the thyroid at any time after injection mainly since the labeled compound can target tumor vasculature with high affinity and specificity and it is stable without iodothyronine. This is consistent with the results of measurement of *in vitro* stability of ^{131}I-scFv. SPECT imaging using ^{131}I-scFv revealed a higher tumor uptake in the mice-bearing TT cell xenograft at 12 h as well as the whole body. With passage of time, no obvious contrast was observed between the tumor and other tissues, concentration of radioactivity in the tumor decreased, but the rate of decline was slower than the body tissues. At 48 h, tumor imaging was mostly clear mainly due to the contrast as compared with the whole body. Hence, SPECT-CT imaging fusion which shows the tumor site clearly, was performed. The results of biodistribution suggested that the radio-labeled probe can particularly accumulate in tumor tissues.

In conclusion, the biological characteristics, *in vitro* stability, biodistribution and imaging properties of ^{131}I-scFv were evaluated. High tumor uptake and retention suggested that this radio-labeled peptide has the potential to be used as a molecular probe for imaging tumor angiogenesis in MTC. The use of ^{131}I-scFv in diagnosing different types of malignant tumors is expected to be explored.

Acknowledgements

The present study was funded by the National Natural Science Foundation of China (no. 81071171).

References

1. Cerrato A, De Falco V and Santoro M: Molecular genetics of medullary thyroid carcinoma: The quest for novel therapeutic targets. J Mol Endocrinol 43: 143-155, 2009.
2. Gilliland FD, Hunt WC, Morris DM and Key CR: Prognostic factors for thyroid carcinoma. A population-based study of 15,698 cases from the Surveillance, Epidemiology and End Results (SEER) program 1973-1991. Cancer 79: 564-573, 1997.
3. Monson JP: The epidemiology of endocrine tumours. Endocr Relat Cancer 7: 29-36, 2000.
4. Kudo T, Miyauchi A, Ito Y, Takamura Y, Amino N and Hirokawa M: Diagnosis of medullary thyroid carcinoma by calcitonin measurement in fine-needle aspiration biopsy specimens. Thyroid 17: 635-638, 2007.
5. Jo VY, Renshaw AA and Krane JF: Relative sensitivity of thyroid fine-needle aspiration by tumor type and size. Diagn Cytopathol 41: 871-875, 2013.
6. Trimboli P, Cremonini N, Ceriani L, Saggiorato E, Guidobaldi L, Romanelli F, Ventura C, Laurenti O, Messuti I, Solaroli E, *et al*: Calcitonin measurement in aspiration needle washout fluids has higher sensitivity than cytology in detecting medullary thyroid cancer: A retrospective multicentre study. Clin Endocrinol 80: 135-140, 2014.
7. Pusztaszeri MP, Bongiovanni M and Faquin WC: Update on the cytologic and molecular features of medullary thyroid carcinoma. Adv Anat Pathol 21: 26-35, 2014.
8. Trimboli P, Treglia G, Guidobaldi L, Romanelli F, Nigri G, Valabrega S, Sadeghi R, Crescenzi A, Faquin WC, Bongiovanni M, *et al*: Detection rate of FNA cytology in medullary thyroid carcinoma: A meta-analysis. Clin Endocrinol 82: 280-285, 2015.
9. Essig GF Jr, Porter K, Schneider D, Debora A, Lindsey SC, Busonero G, Fineberg D, Fruci B, Boelaert K, Smit JW, *et al*: Fine needle aspiration and medullary thyroid carcinoma: The risk of inadequate preoperative evaluation and initial surgery when relying upon FNAB cytology alone. Endocr Pract 19: 920-927, 2013.
10. Lee S, Shin JH, Han BK and Ko EY: Medullary thyroid carcinoma: Comparison with papillary thyroid carcinoma and application of current sonographic criteria. AJR Am J Roentgenol 194: 1090-1094, 2010.
11. Choi N, Moon WJ, Lee JH, Baek JH, Kim DW and Park SW: Ultrasonographic findings of medullary thyroid cancer: Differences according to tumor size and correlation with fine needle aspiration results. Acta Radiol 52: 312-316, 2011.
12. Kim SH, Kim BS, Jung SL, Lee JW, Yang PS, Kang BJ, Lim HW, Kim JY, Whang IY, Kwon HS, *et al*: Ultrasonographic findings of medullary thyroid carcinoma: A comparison with papillary thyroid carcinoma. Korean J Radiol 10: 101-105, 2009.
13. Trimboli P, Nasrollah N, Amendola S, Rossi F, Ramacciato G, Romanelli F, Aurello P, Crescenzi A, Laurenti O, Condorelli E, *et al*: Should we use ultrasound features associated with papillary thyroid cancer in diagnosing medullary thyroid cancer? Endocr J 59: 503-508, 2012.
14. Andrioli M, Trimboli P, Amendola S, Valabrega S, Fukunari N, Mirella M and Persani L: Elastographic presentation of medullary thyroid carcinoma. Endocrine 45: 153-155, 2014.
15. Fukushima M, Ito Y, Hirokawa M, Miya A, Kobayashi K, Akasu H, Shimizu K and Miyauchi A: Excellent prognosis of patients with nonhereditary medullary thyroid carcinoma with ultrasonographic findings of follicular tumor or benign nodule. World J Surg 33: 963-968, 2009.
16. Trimboli P, Giovanella L, Valabrega S, Andrioli M, Baldelli R, Cremonini N, Rossi F, Guidobaldi L, Barnabei A, Rota F, *et al*: Ultrasound features of medullary thyroid carcinoma correlate with cancer aggressiveness: A retrospective multicenter study. J Exp Clin Cancer Res 33: 87, 2014.
17. Trimboli P and Giovanella L: Serum calcitonin negative medullary thyroid carcinoma: A systematic review of the literature. Clin Chem Lab Med 53: 1507-1514, 2015.
18. Rubello D, Rampin L, Nanni C, Banti E, Ferdeghini M, Fanti S, Al-Nahhas A and Gross MD: The role of ^{18}F-FDG PET/CT in detecting metastatic deposits of recurrent medullary thyroid carcinoma: A prospective study. Eur J Surg Oncol 34: 581-586, 2008.
19. Goldenberg DM, DeLand F, Kim E, Bennett S, Primus FJ, van Nagell JR Jr, Estes N, DeSimone P and Rayburn P: Use of radiolabeled antibodies to carcinoembryonic antigen for the detection and localization of diverse cancers by external photoscanning. N Engl J Med 298: 1384-1386, 1978.
20. Blottière HM, Steplewski Z, Herlyn D and Douillard JY: Human anti-murine immunoglobulin responses and immune functions in cancer patients receiving murine monoclonal antibody therapy. Hum Antibodies Hybridomas 2: 16-25, 1991.
21. Bird RE, Hardman KD, Jacobson JW, Johnson S, Kaufman BM, Lee SM, Lee T, Pope SH, Riordan GS and Whitlow M: Single-chain antigen-binding proteins. Science 242: 423-426, 1988.
22. Subedi GP, Satoh T, Hanashima S, Ikeda A, Nakada H, Sato R, Mizuno M, Yuasa N, Fujita-Yamaguchi Y and Yamaguchi Y: Overproduction of anti-Tn antibody MLS128 single-chain Fv fragment in *Escherichia coli* cytoplasm using a novel pCold-PDI vector. Protein Expr Purif 82: 197-204, 2012.
23. Marasco WA and Dana Jones S: Antibodies for targeted gene therapy: Extracellular gene targeting and intracellular expression. Adv Drug Deliv Rev 31: 153-170, 1998.
24. Leyton JV, Olafsen T, Sherman MA, Bauer KB, Aghajanian P, Reiter RE and Wu AM: Engineered humanized diabodies for microPET imaging of prostate stem cell antigen-expressing tumors. Protein Eng Des Sel 22: 209-216, 2009.
25. Pavlinkova G, Booth BJ, Batra SK and Colcher D: Radioimmunotherapy of human colon cancer xenografts using a dimeric single-chain Fv antibody construct. Clin Cancer Res 5: 2613-2619, 1999.
26. Marks JD, Hoogenboom HR, Bonnert TP, McCafferty J, Griffiths AD and Winter G: By-passing immunization. Human antibodies from V-gene libraries displayed on phage. J Mol Biol 222: 581-597, 1991.
27. Osbourn J, Jermutus L and Duncan A: Current methods for the generation of human antibodies for the treatment of autoimmune diseases. Drug Discov Today 8: 845-851, 2003.
28. Puleo S, Mauro L, Gagliano G, Lombardo R, Li Destri G, Petrillo G and Di Carlo I: Liver damage after transarterial chemoembolization without embolizing agent in unresectable hepatocellular carcinoma. Tumori 89: 285-287, 2003.
29. Chung KY and Saltz LB: Antibody-based therapies for colorectal cancer. Oncologist 10: 701-709, 2005.
30. Staelens S, Desmet J, Ngo TH, Vauterin S, Pareyn I, Barbeaux P, Van Rompaey I, Stassen JM, Deckmyn H and Vanhoorelbeke K: Humanization by variable domain resurfacing and grafting on a human IgG_4, using a new approach for determination of non-human like surface accessible framework residues based on homology modelling of variable domains. Mol Immunol 43: 1243-1257, 2006.
31. Beckmann C, Brittnacher M, Ernst R, Mayer-Hamblett N, Miller SI and Burns JL: Use of phage display to identify potential *Pseudomonas aeruginosa* gene products relevant to early cystic fibrosis airway infections. Infect Immun 73: 444-452, 2005.
32. Sidhu SS, Lowman HB, Cunningham BC and Wells JA: Phage display for selection of novel binding peptides. Methods Enzymol 328: 333-363, 2000.
33. Hegmans JP, Radosevic K, Voerman JS, Burgers JA, Hoogsteden HC and Prins JB: A model system for optimising the selection of membrane antigen-specific human antibodies on intact cells using phage antibody display technology. J Immunol Methods 262: 191-204, 2002.
34. Foy BD, Killeen GF, Frohn RH, Impoinvil D, Williams A and Beier JC: Characterization of a unique human single-chain antibody isolated by phage-display selection on membrane-bound mosquito midgut antigens. J Immunol Methods 261: 73-83, 2002.